Supporting Information

Synthesis and Characterization of Light-driven Dithienylcyclopentene Switches with Axial Chirality

Yannian Li[†]*, Augustine Urbas*[§]*, and Quan Li*[*,†]

[†]Liquid Crystal Institute, Kent State University, Kent, Ohio 44242, United States; [§]Materials and Manufacturing Directorate, Air Force Research Laboratory WPAFB, Ohio 45433, United States

Contents:

1. CD spectra of (*S*)-12a, (*R*)-12b, (*S*)-12c, (*S*)-13a, (*R*)-13b, (*S*)-13c, (*S*,*S*)-1a, (*R*,*R*)-1b

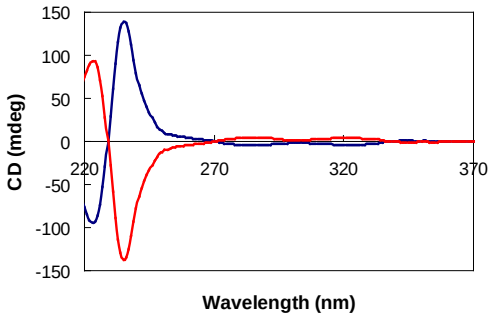

Figure S1. CD spectra of (*S*)-**12a** (blue) and (*R*)-**12b** (red) in hexane (15 µM)

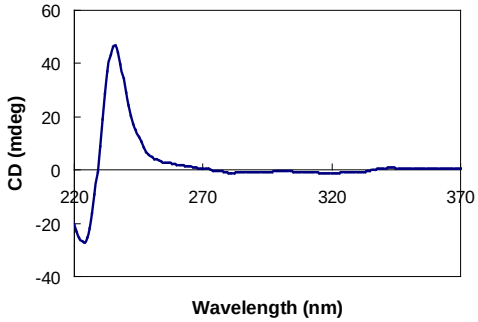

Figure S2. CD spectra of (*S*)-**12c** in hexanes (5 µM)

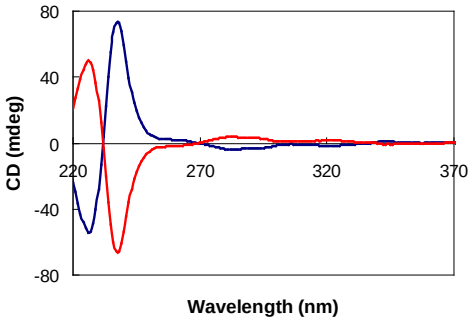

Figure S3. CD spectra of (*S*)-**13a** (blue) and (*R*)-**13b** (red) in hexane (7 µM)

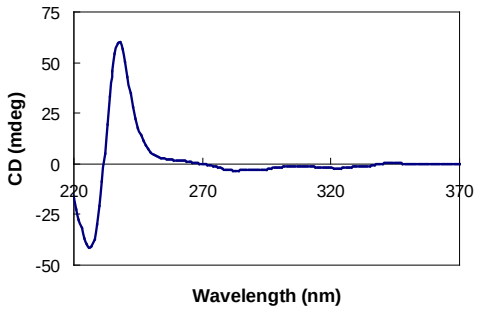

Figure S4. CD spectra of (*S*)-**13c** in hexane (5 µM)

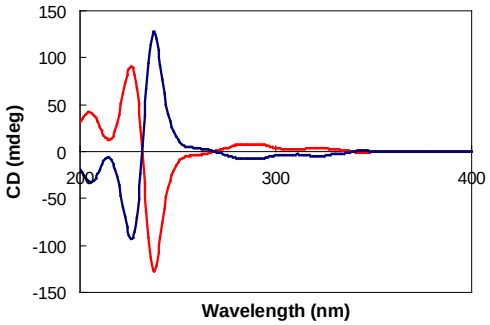

Figure S5. CD spectra of (*R*,*R*)-**1a** (blue) and (*S*,*S*)-**1b** (red) in hexane (15 µM)

2. ^{1}H NMR changes of (*S*,*S*)-1a before and after UV irradiation

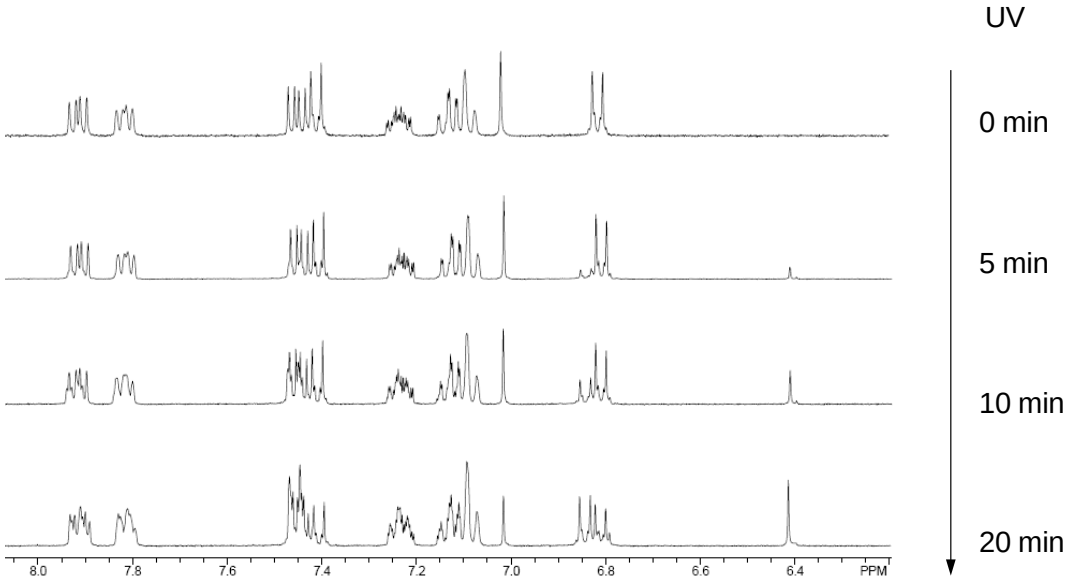

Figure S6. Aromatic region for ^{1}H NMR changes of 2 mg (*S*,*S*)-**1a** in 0.5 ml THF-*d8* upon UV irradiation at 290 nm (30 mW/cm^{2}) for 5 min, 10 min and 20 min.

3. Photoisomerization of (*S*,*S*)-1a.

The photoisomerization of (*S*,*S*)-**1a** generated two new chiral centers in the closed form. Since the photocyclization proceed only from the antiparallel style of two thiophene rings, the configurations of these two chiral centers are (*S*,*S*) or (*R*,*R*). Together with the axial chirality from binaphthyl, the closed form has two diastereomers with the configurations of (*S*,*S*,*S*,*S*) and (*S*,*R*,*R*,*S*).

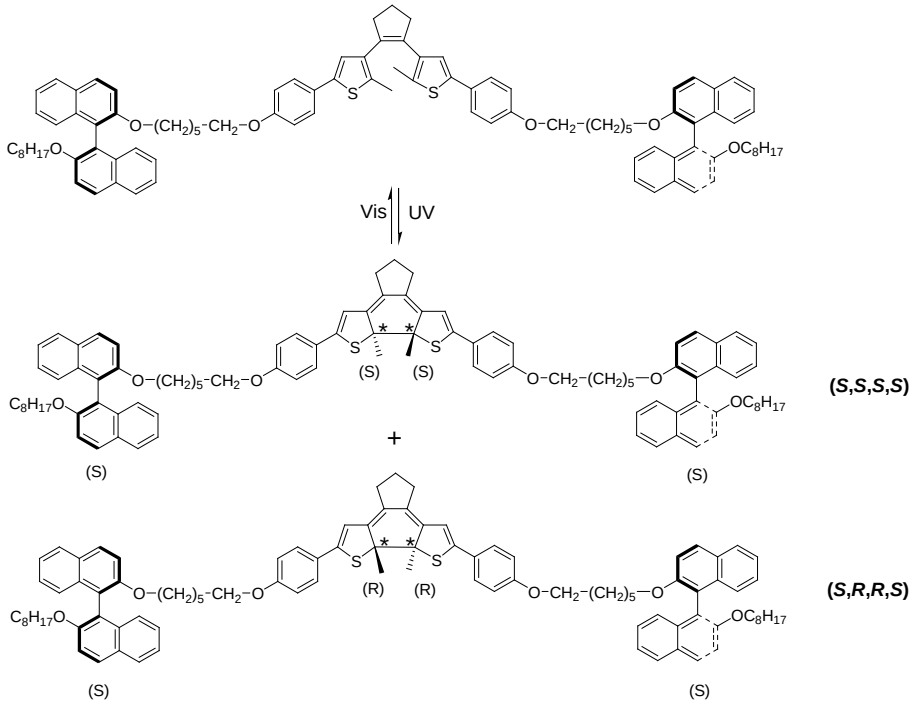

Figure S7. Photoisomerization of (*S*,*S*)-**1a**.

4. Measurement of pitch and helical twisting power

A conventional technique for pitch measurement is Grandjean-Cano wedge method[1]. Such wedge cell with an opening angle θ is made by applying two differently sized spacers at each end of the cell (Figure S7). If the alignment of the substrates is planar (the director lies parallel to the surface) and the rubbing directions of the substrates are parallel to one another, the cholesteric LC becones discrete. Because the value of the pitch is fixed, and the alignment is also fixed, the cholesteric LC arranges itself as in Figure S7. This arrangement produces disclination lines between areas that contain a different number of layers. The difference in thickness between each domain must be $p/2$ in order to satisfy the alignment boundary

condition.

The disclination lines of the cholesteric liquid crystal in the wedge cell can be seen through a polarizing optical microscope. The pitch was determined according to the equation $p = 2R \tan\theta$, where R represents the distance between the Grandjean lines and θ is the wedge angle of wedge cells (EHC, KCRK-07, $\tan\theta = 0.0196$). The inverse of pitch proportionally increases with increase in the concentration of a chiral dopant and HTP values is $\beta = 1/(pc)$, where β is the helical twisting power, i.e. the ability of the chiral dopant to twist a nematic LC, and is the concentration of the chiral dopant.

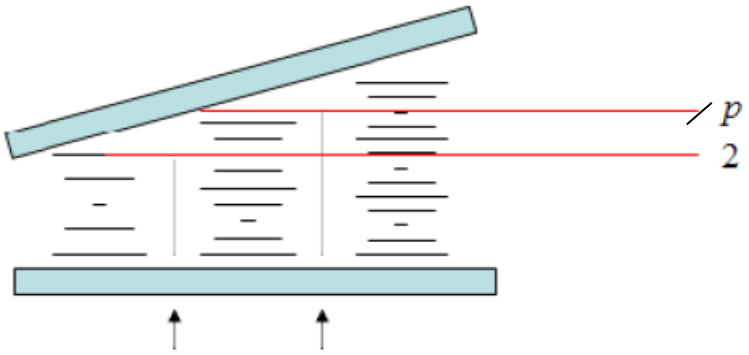

Figure S8. Schematic illustation of a Grandjean-Cano wedge cell for the pitch measurement of cholesteric LC. Disclination lines are pointed out with arrows and the thickness change between two domains is marked $p/2$.

The chiral nematic liquid crystal was prepared by weighing appropriate amount of host liquid crystal and the dopant into a vial followed by mixing them with the addition of a few drops of dichloromethane. After evaporation of the solvent under reduced pressure, the mixture was loaded into the wedge cell by capillary action at room temperature. The pitch was then determined by measuring the intervals of Cano's lines appearing on the surfaces of wedge-type liquid crystalline cells. Three different concentrations were used by this method for each sample, and the HTP were determined by plotting $1/p$ (μm^{-1}) against concentration of the dopant c (mol%) according to the equation $\beta = 1/(pc)$ (Figure S8).

1. (a) Grandjean, F. *C. R. Hebd. Seances Acad. Sci.* **1921**, *172*, 71. (b) Cano, R. *Bull. Soc. Fr. Mineral.* **1968**, *91*, 20.

(c) Heppke, G.; Oestreicher, F. *Mol. Cryst. Liq. Cryst.* **1978**, *41*, 245-249.

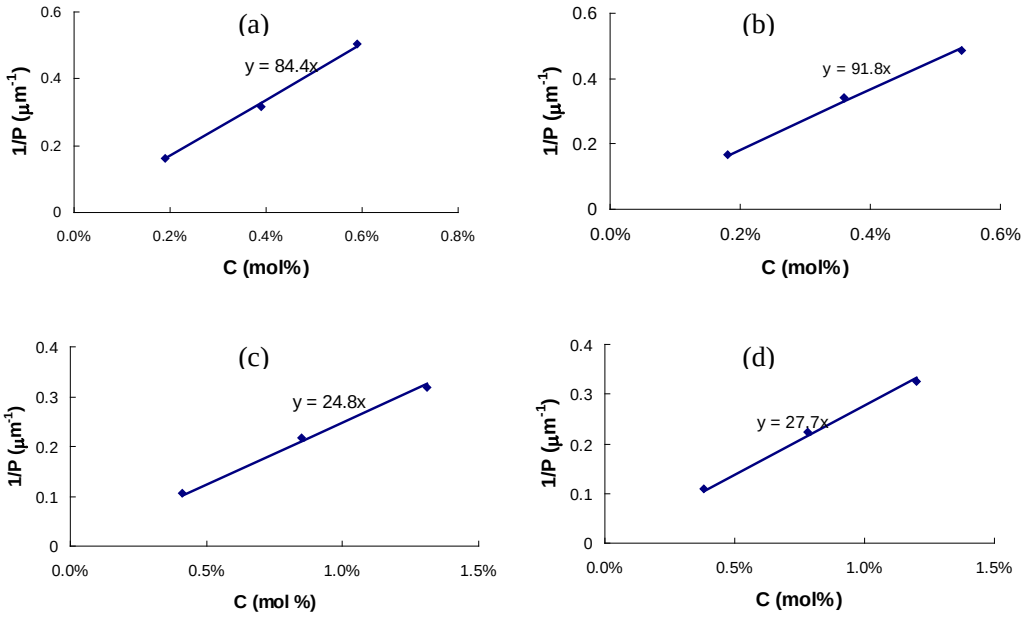

Figure S9. Reciprocal helical pitch as a function of concentration of (*S*, *S*)-**1a** in E7 (a), 5CB (b), and (*S*, *S*)-**2** in E7 (c), in 5CB (d).

5. Copies of ^{1}H NMR and ^{13}C NMR

Compound 7:

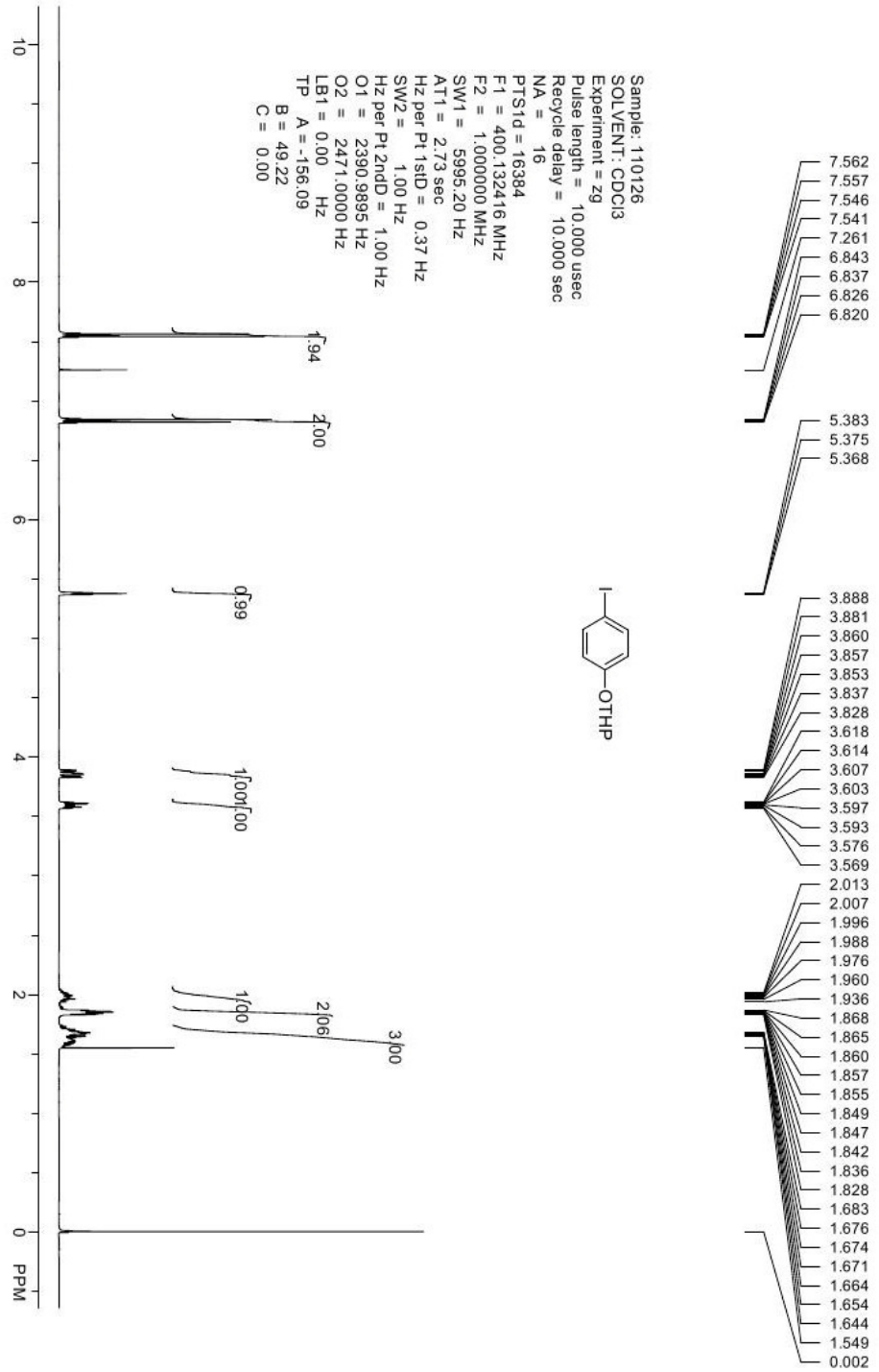

Figure S10. ^{1}H NMR (400 MHz) of **7** in $CDCl_3$.

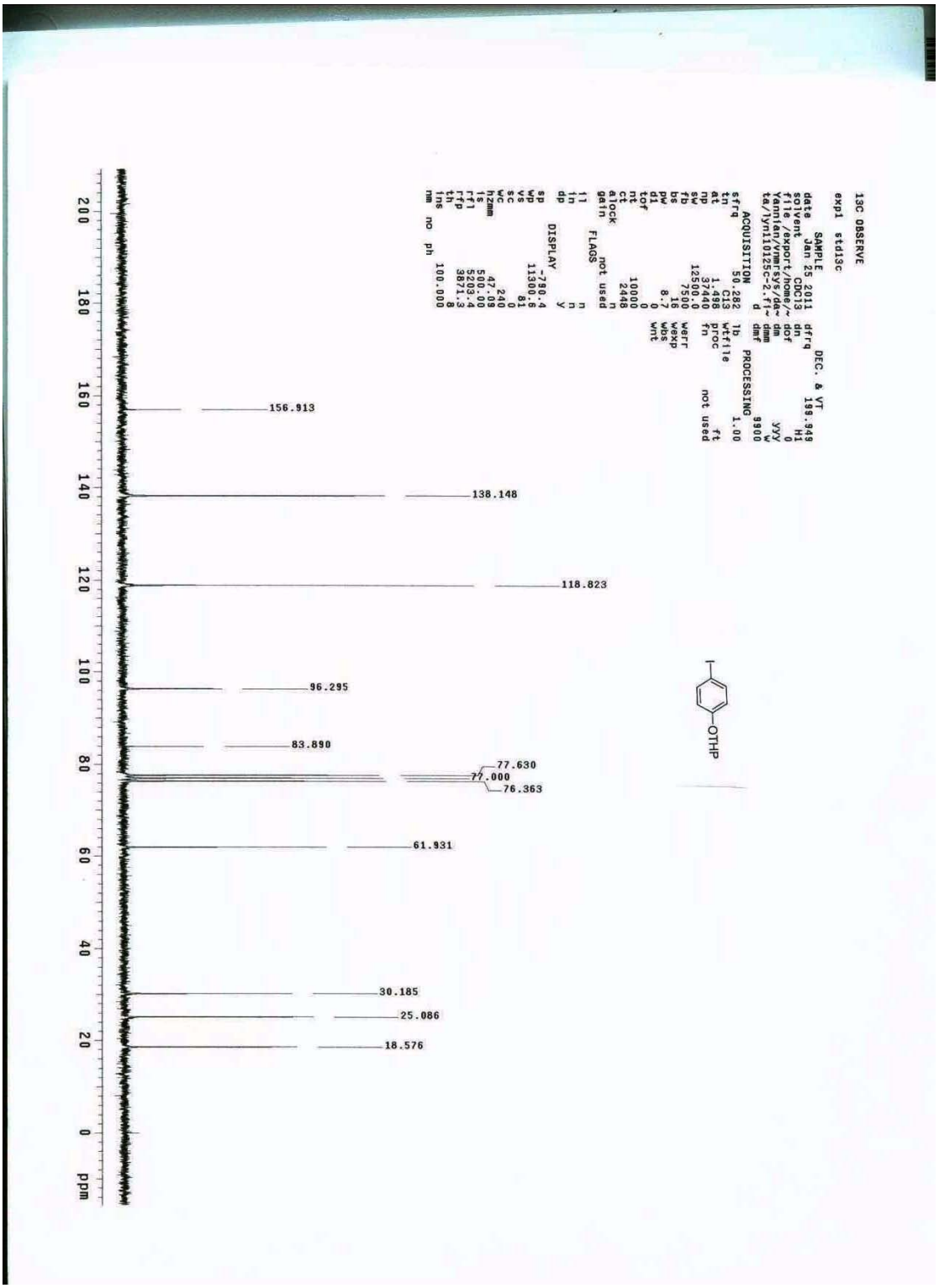

Figure S11. ^{13}C NMR (50 MHz) of **7** in $CDCl_3$.

Compound 8:

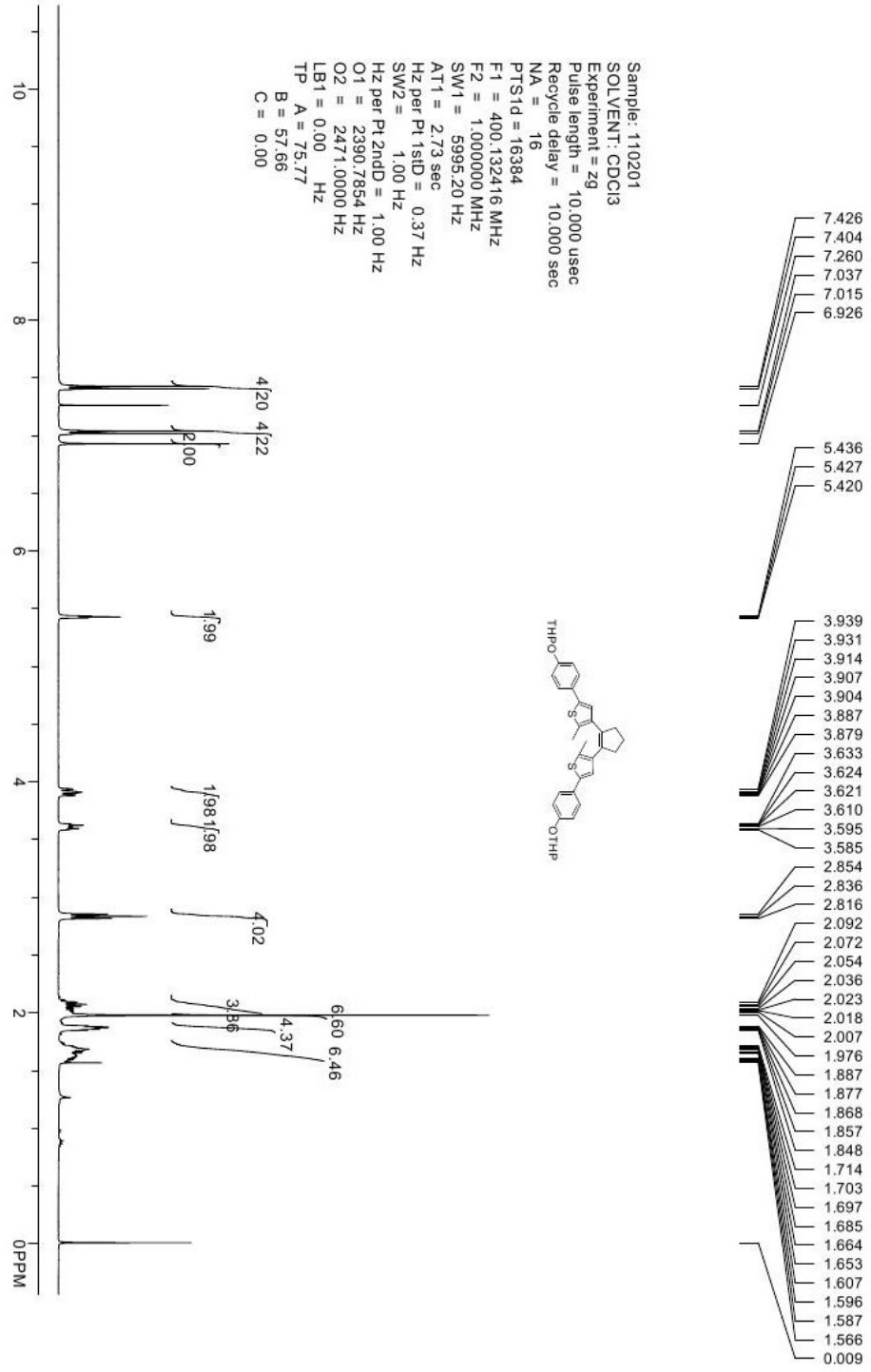

Figure S12. ^{1}H NMR (400 MHz) of **8** in $CDCl_3$.

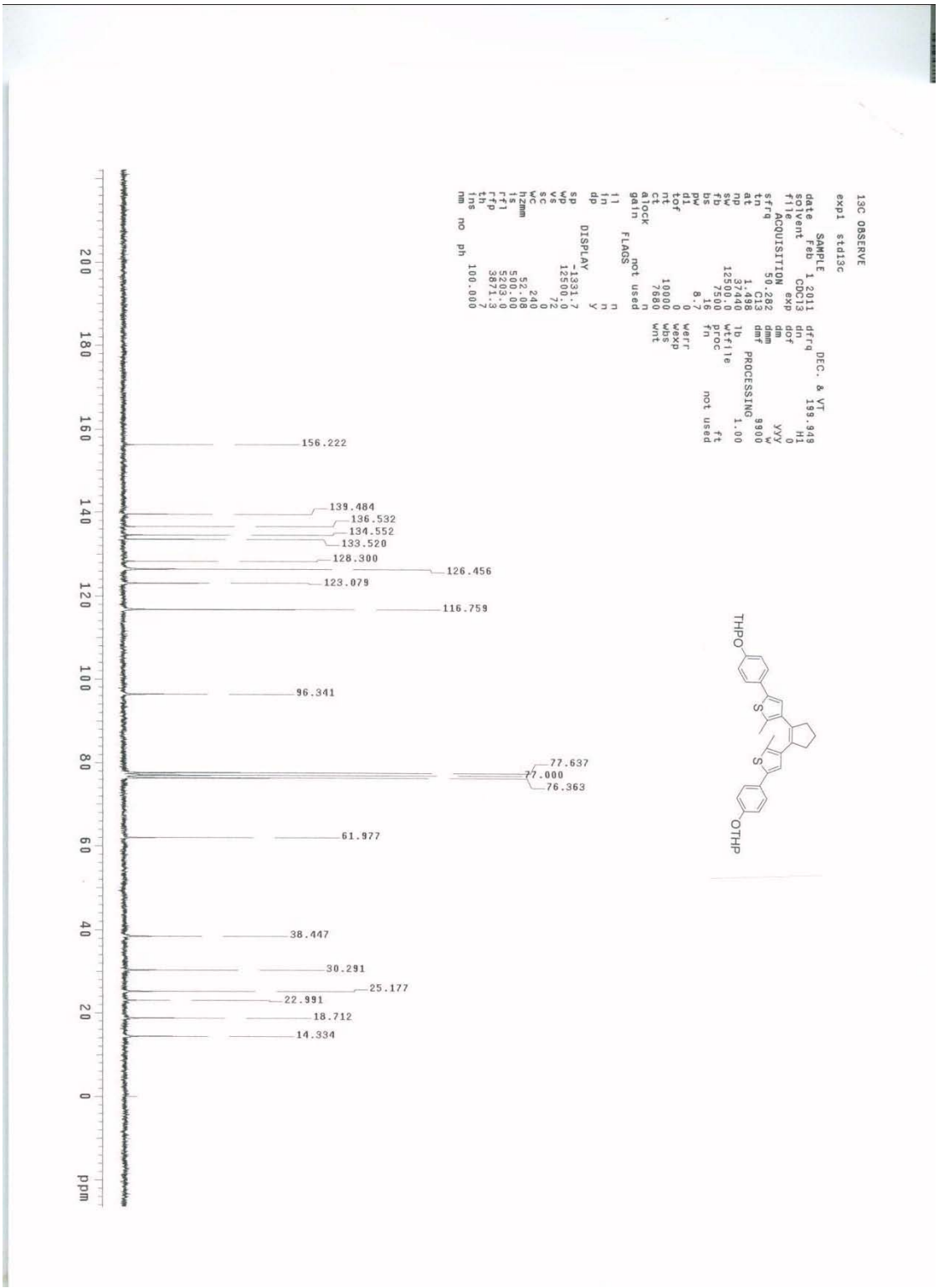

Figure S13. ^{13}C NMR (50 MHz) of **8** in $CDCl_3$.

Compound 9:

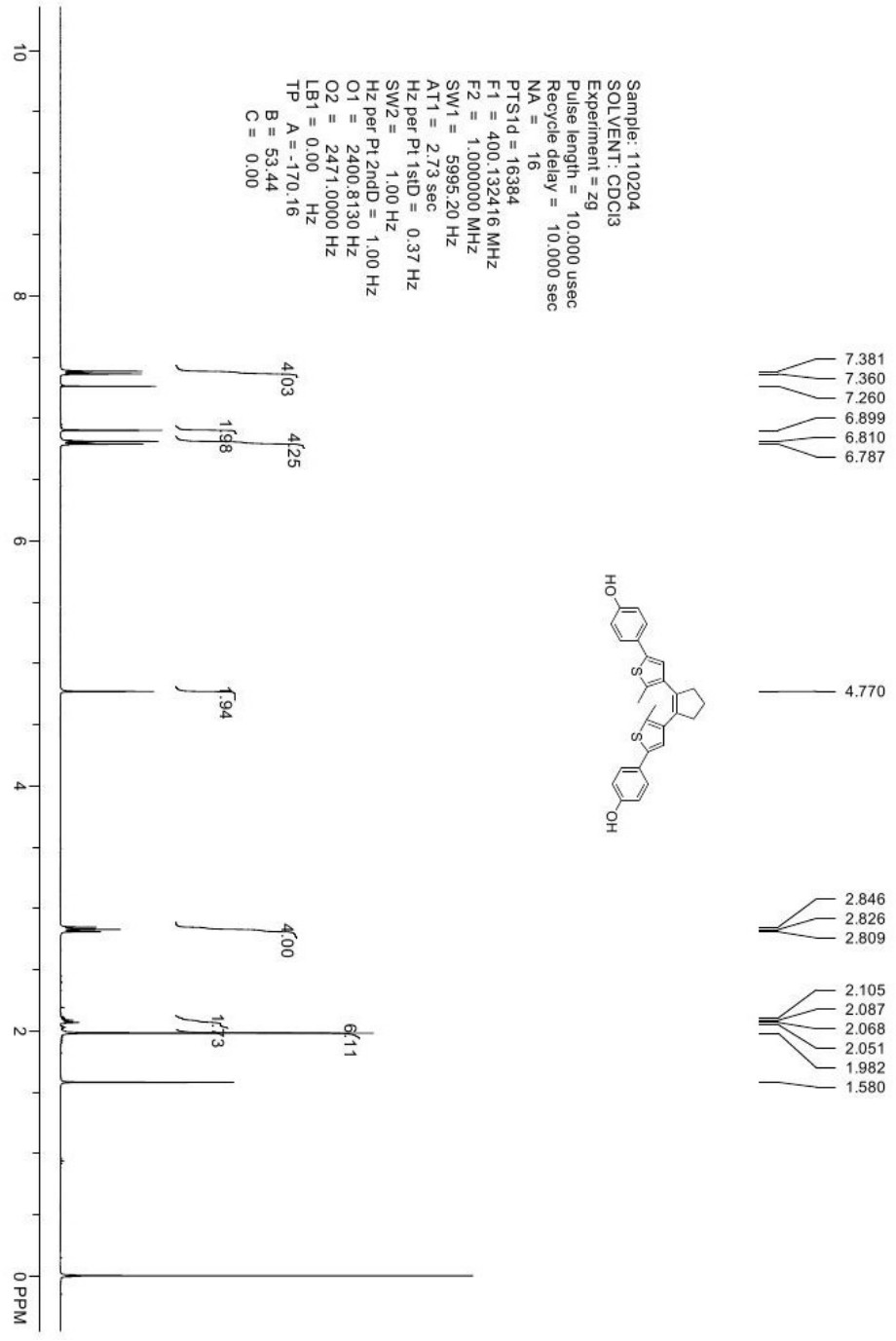

Figure S14. ^{1}H NMR (400 MHz) of **9** in $CDCl_3$.

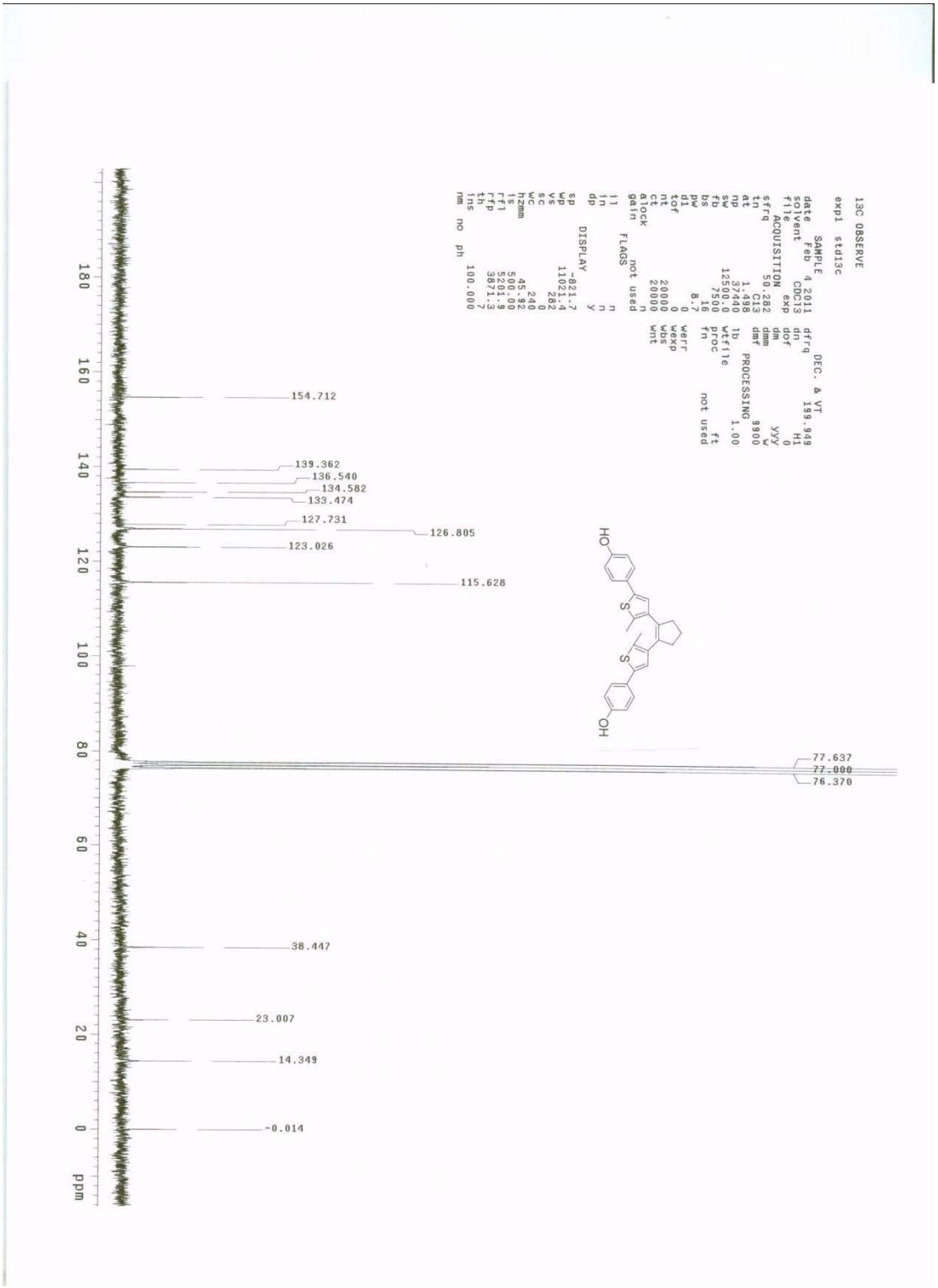

Figure S15. ^{13}C NMR (50 MHz) of **9** in $CDCl_3$.

Compound (*R*)-12b:

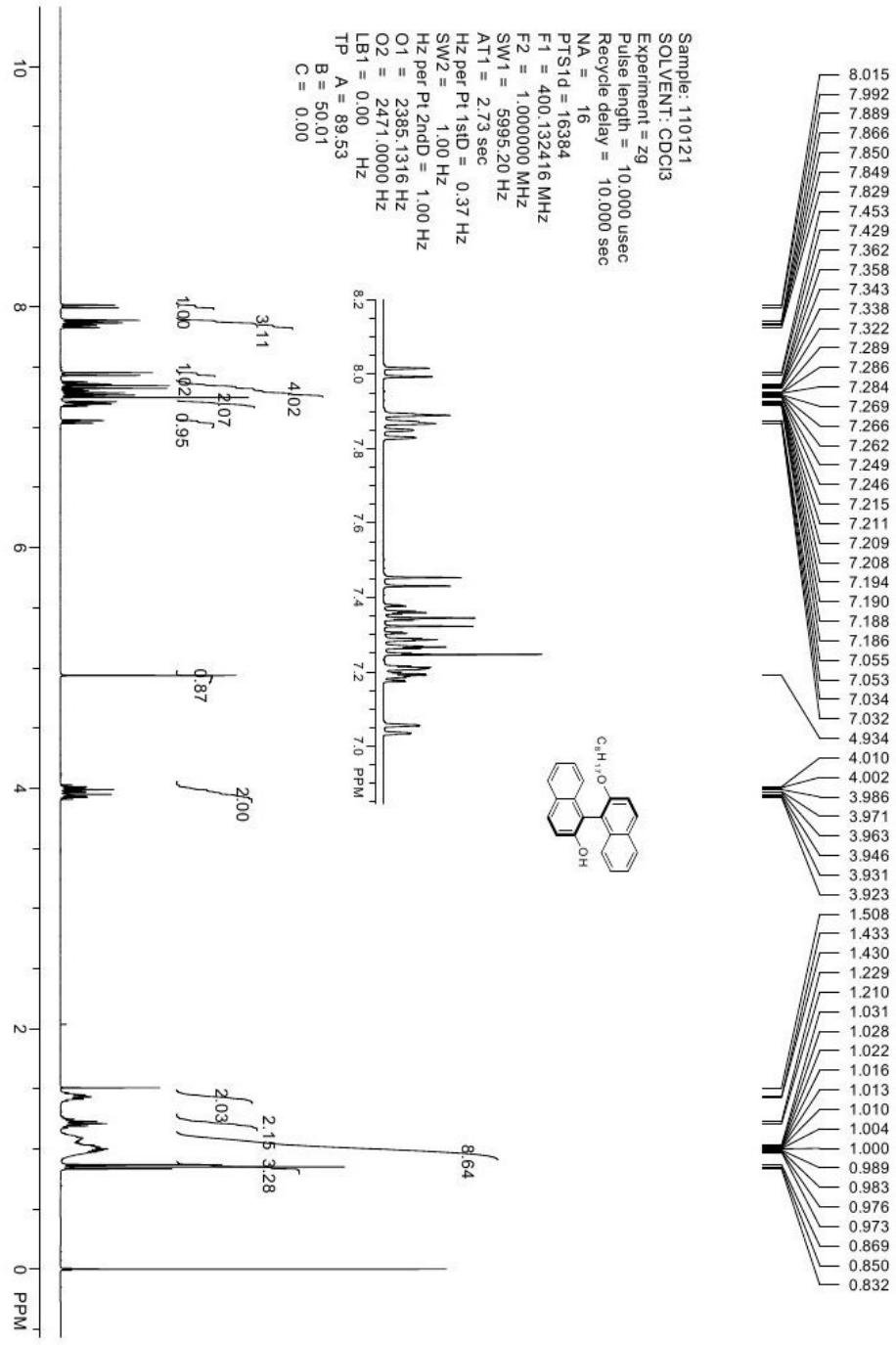

Figure S16. ^{1}H NMR (400 MHz) of (*R*)-**12b** in $CDCl_3$.

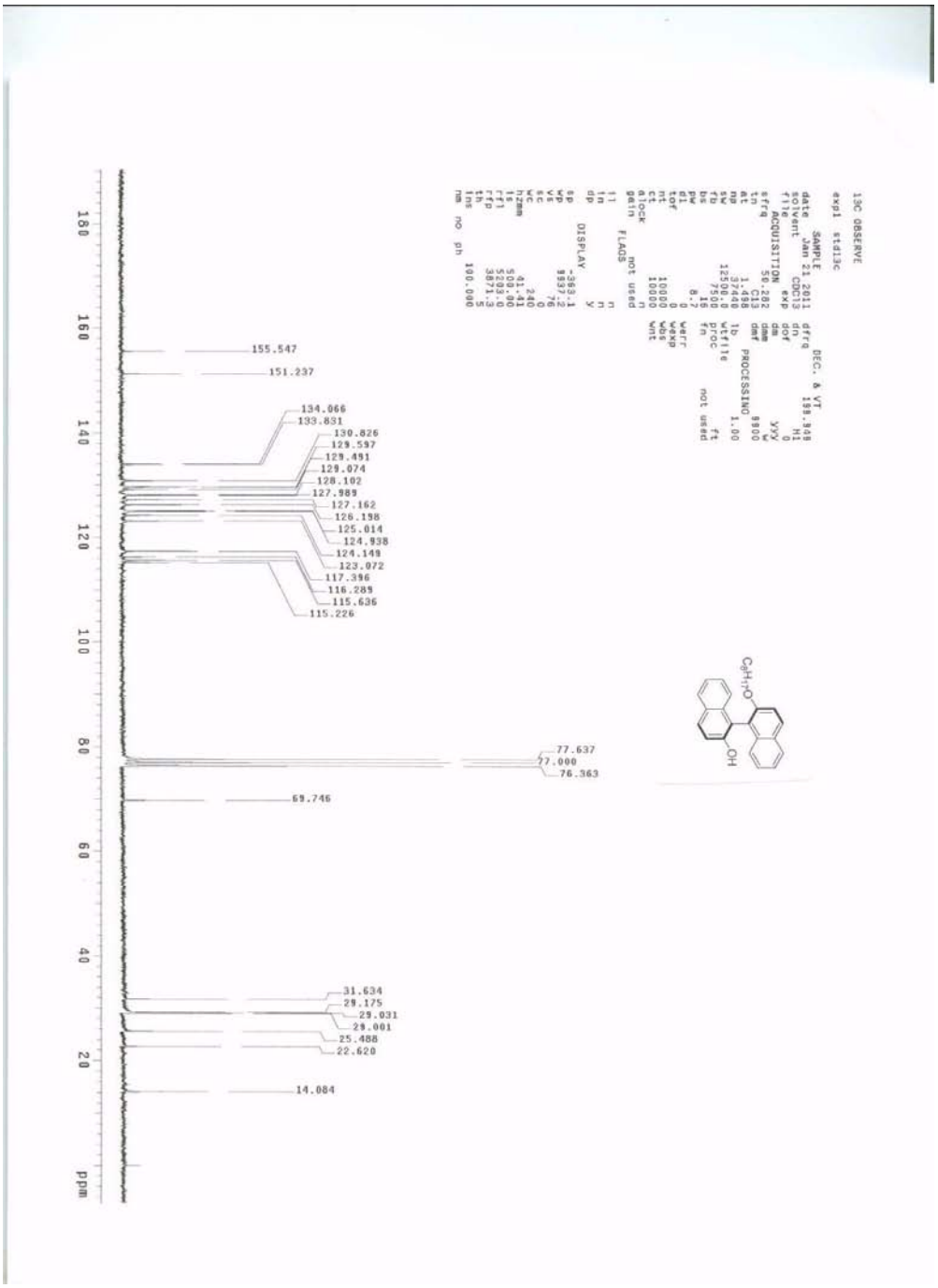

Figure S17. ^{13}C NMR (50 MHz) of (*R*)-**12b** in $CDCl_3$.

Compound (*R*)-13b:

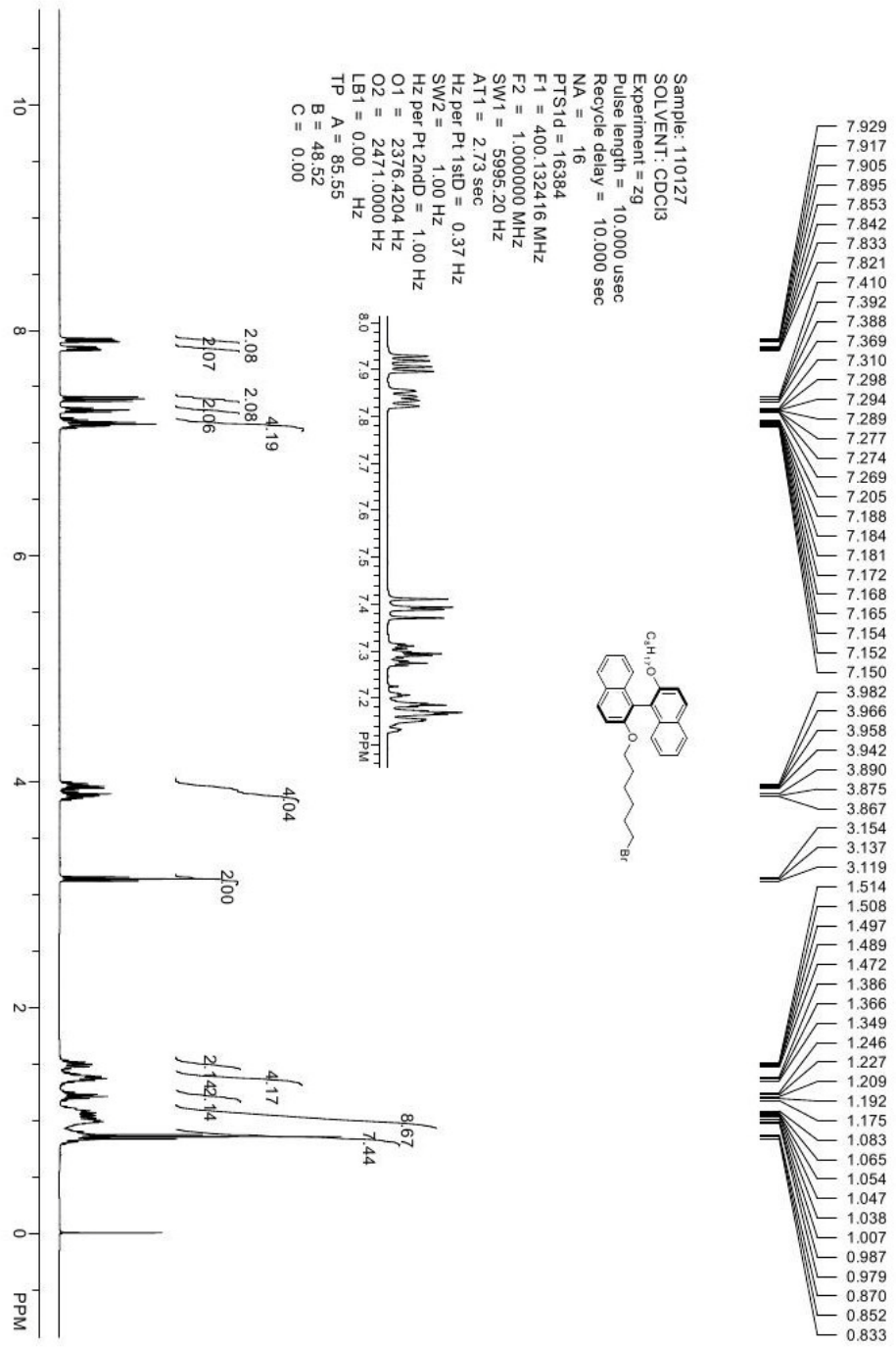

Figure S18. ^{1}H NMR (400 MHz) of **(*R*)-13b** in $CDCl_3$.

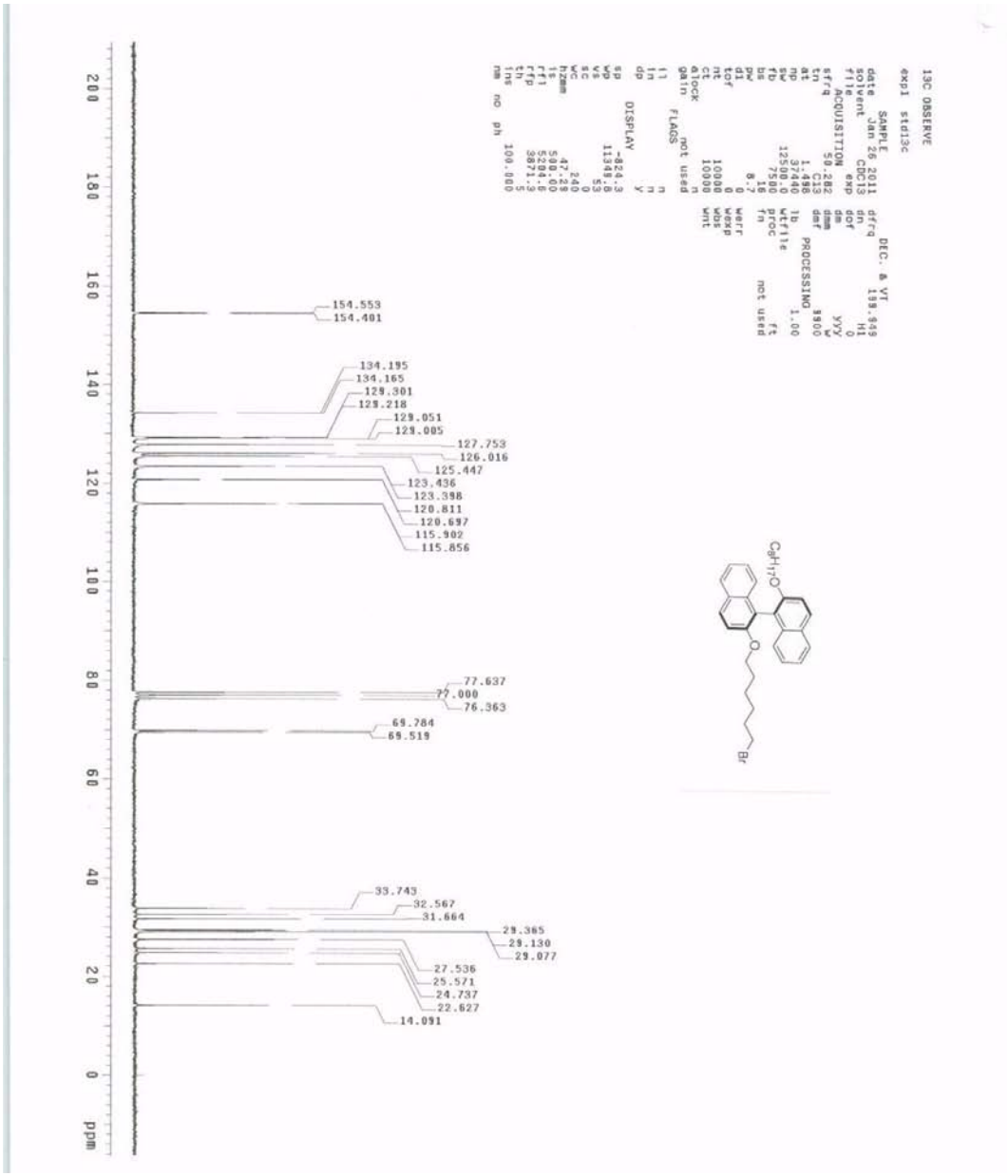

Figure S19. ^{13}C NMR (50 MHz) of (*R*)-**13b** in $CDCl_3$.

Compound 11:

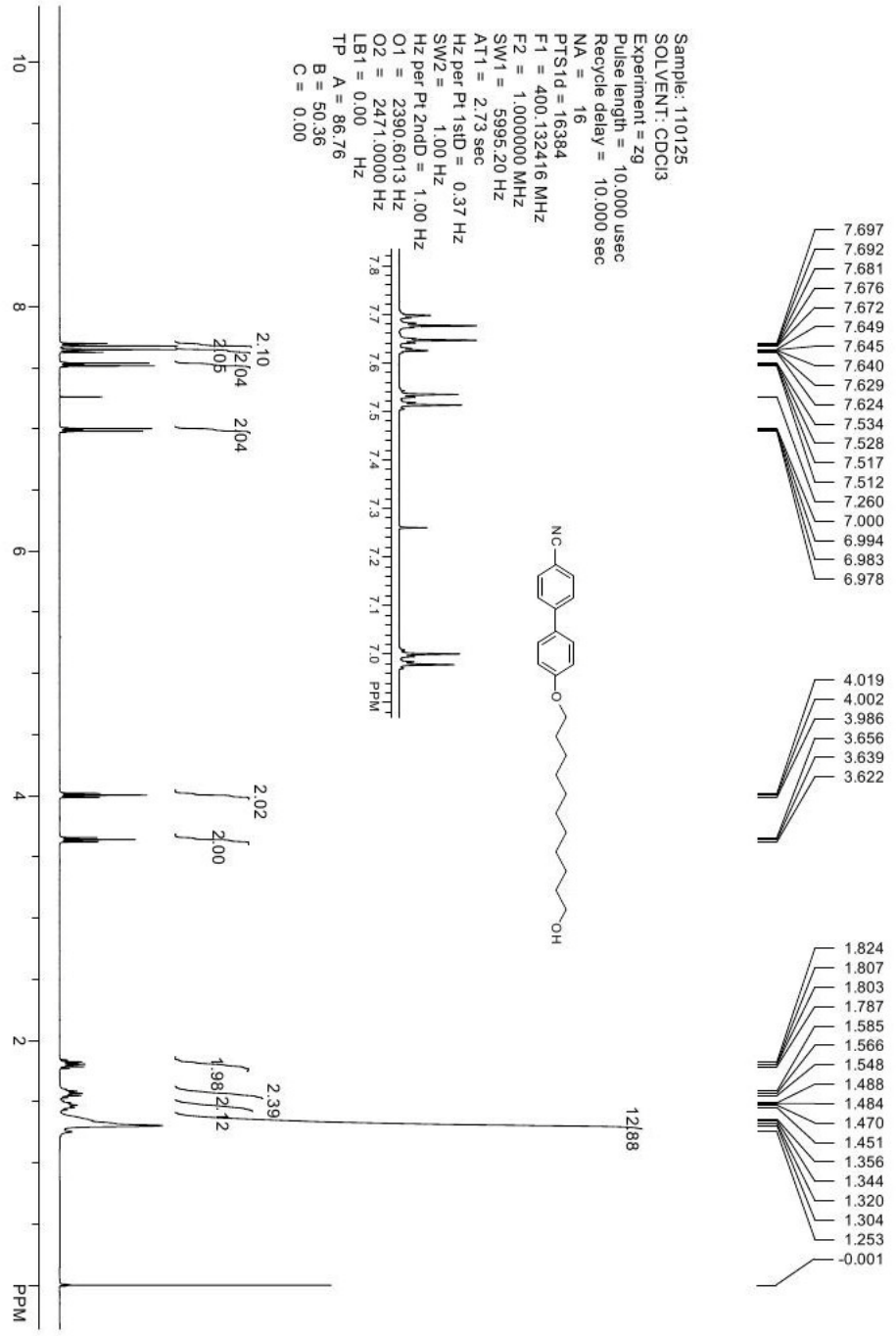

Figure S20. ^{1}H NMR (400 MHz) of **11** in $CDCl_3$.

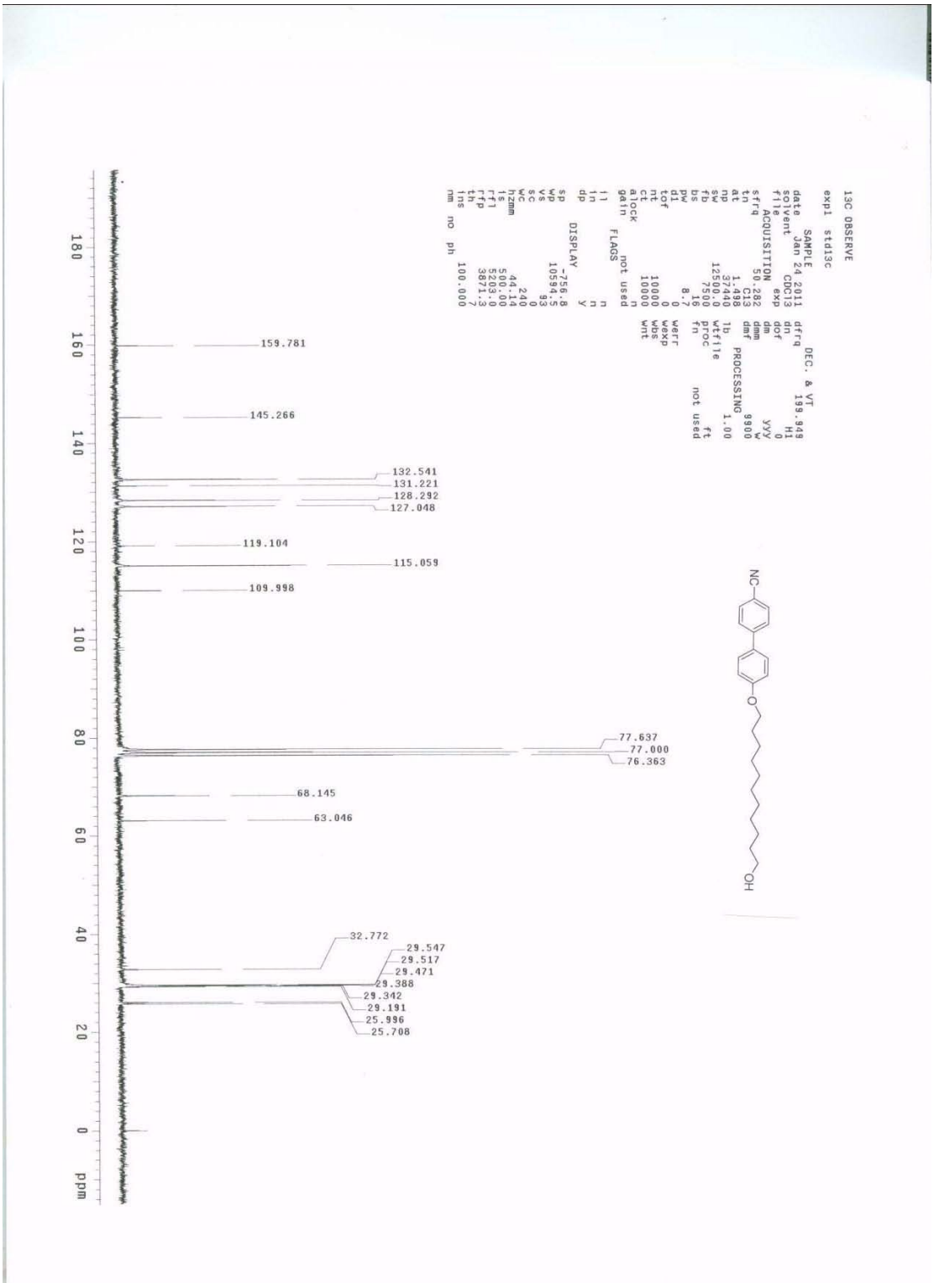

Figure S21. ^{13}C NMR (50 MHz) of **11** in $CDCl_3$.

Compound (*S*)-12c:

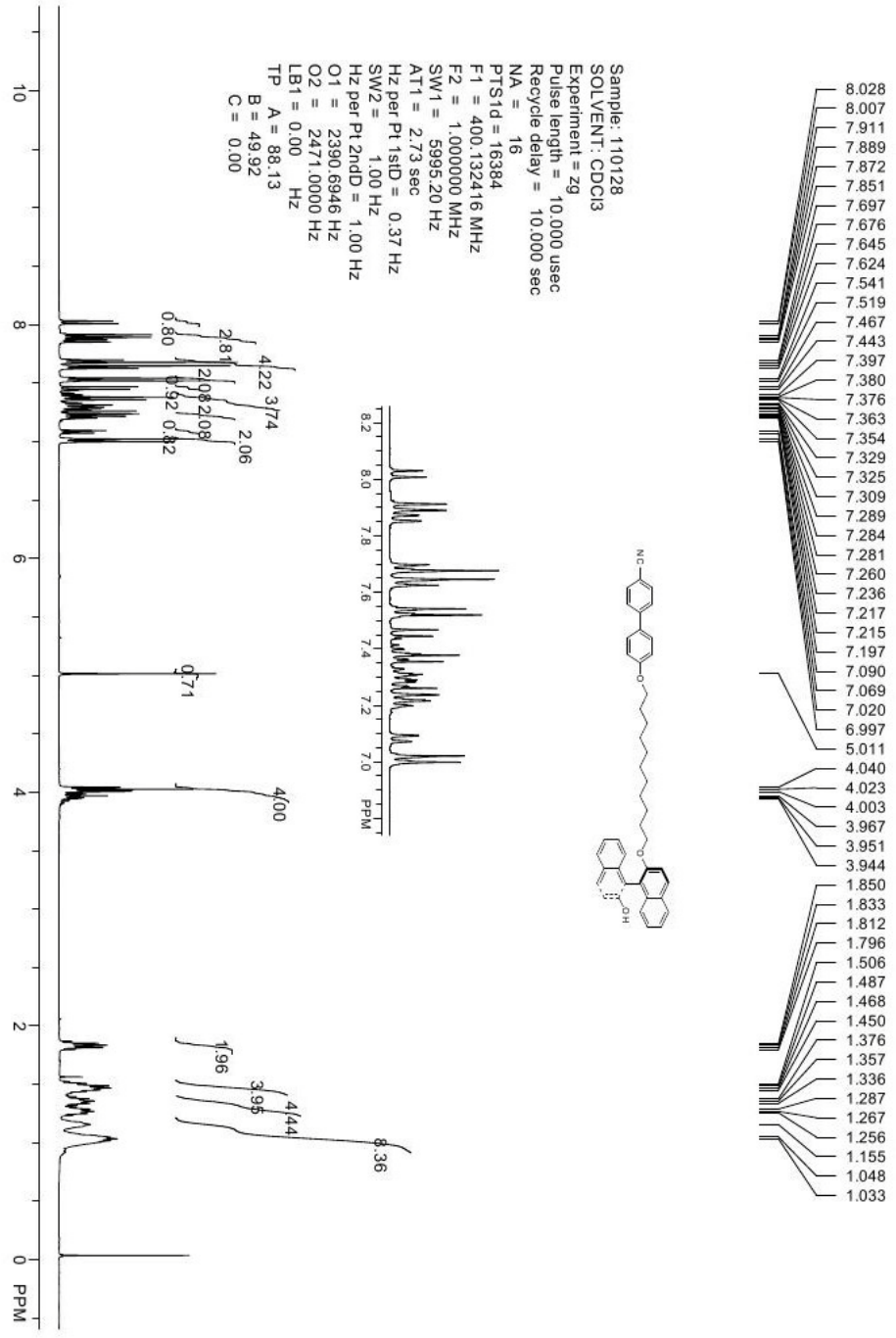

Figure S22. ^{1}H NMR (400 MHz) of **(*S*)-12c** in $CDCl_3$.

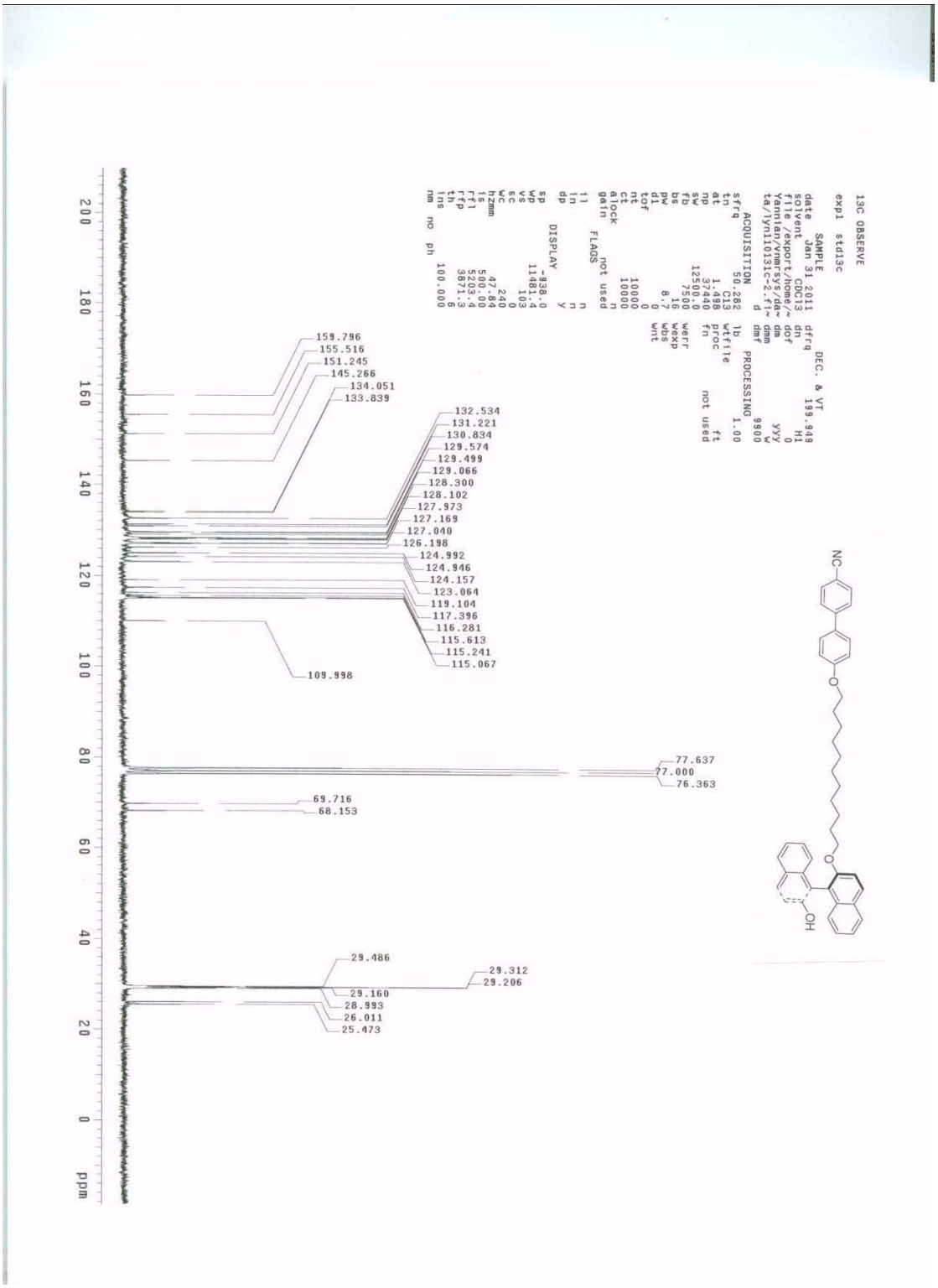

Figure S23. ^{13}C NMR (50 MHz) of **(*S*)-12c** in $CDCl_3$.

Compound (*S*)-13c:

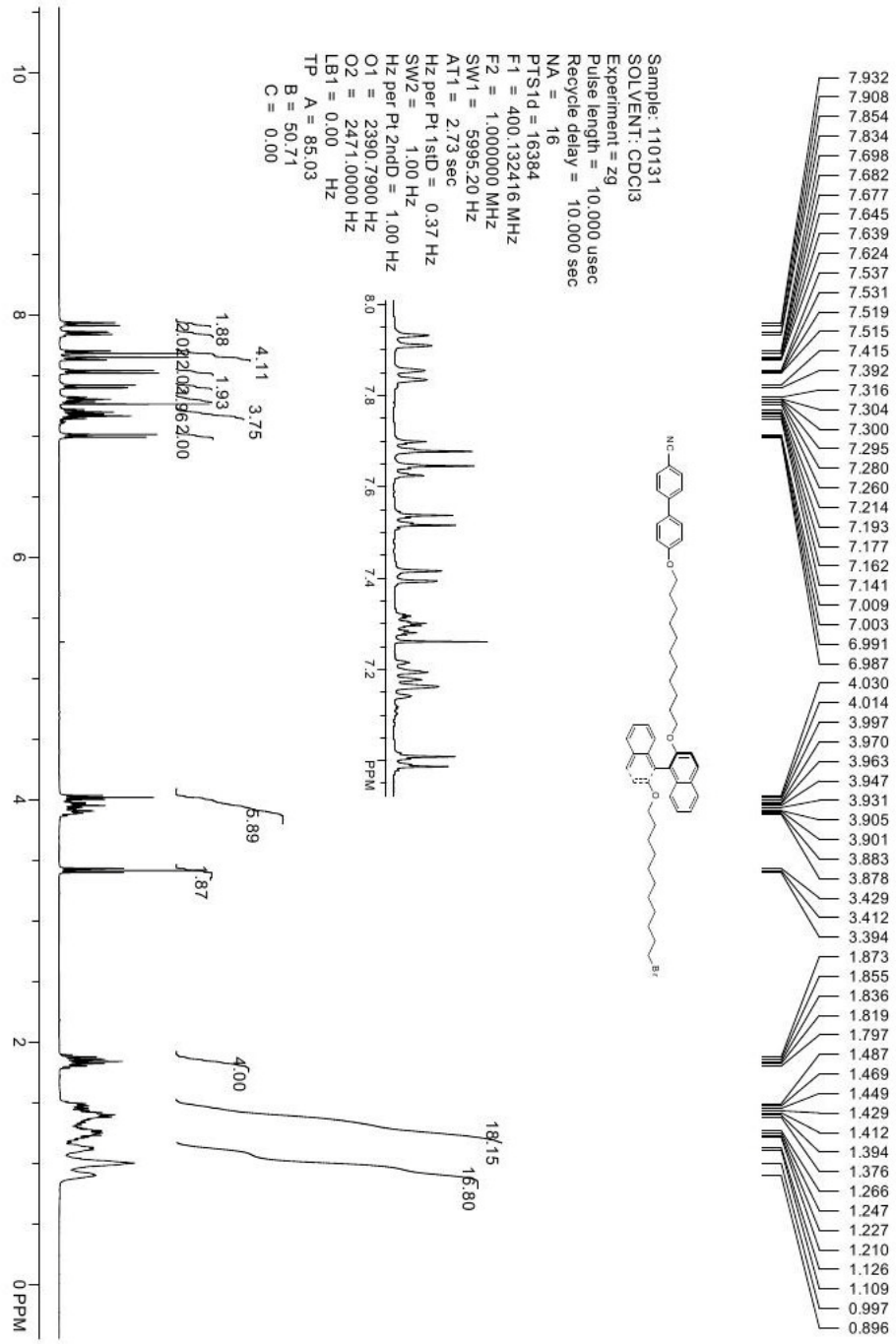

Figure S24. ^{1}H NMR (400 MHz) of **(*S*)-13c** in $CDCl_3$.

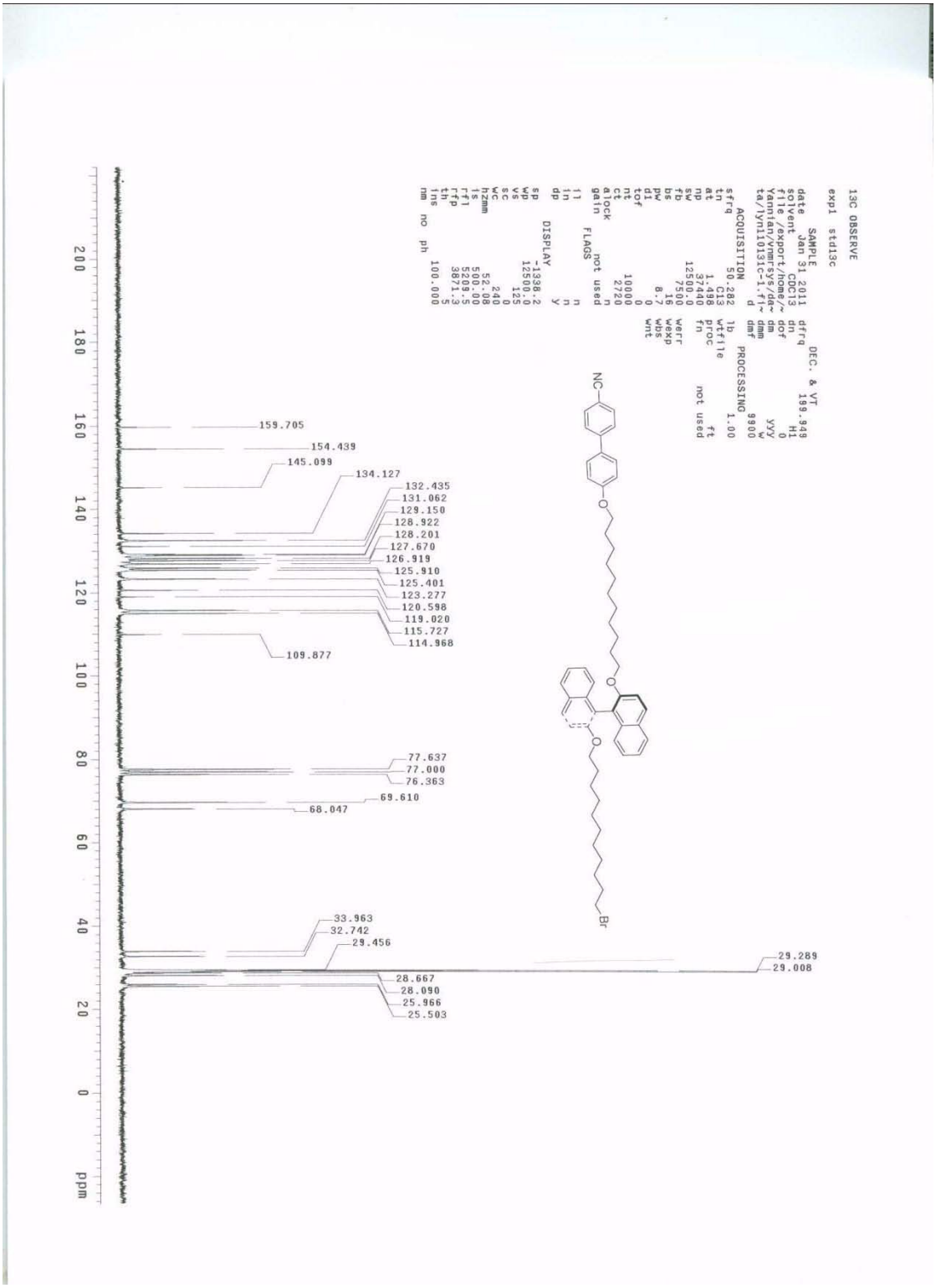

Figure S25. ^{13}C NMR (50 MHz) of **(*S*)-13c** in $CDCl_3$.

Compound (*S*,*S*)-1a:

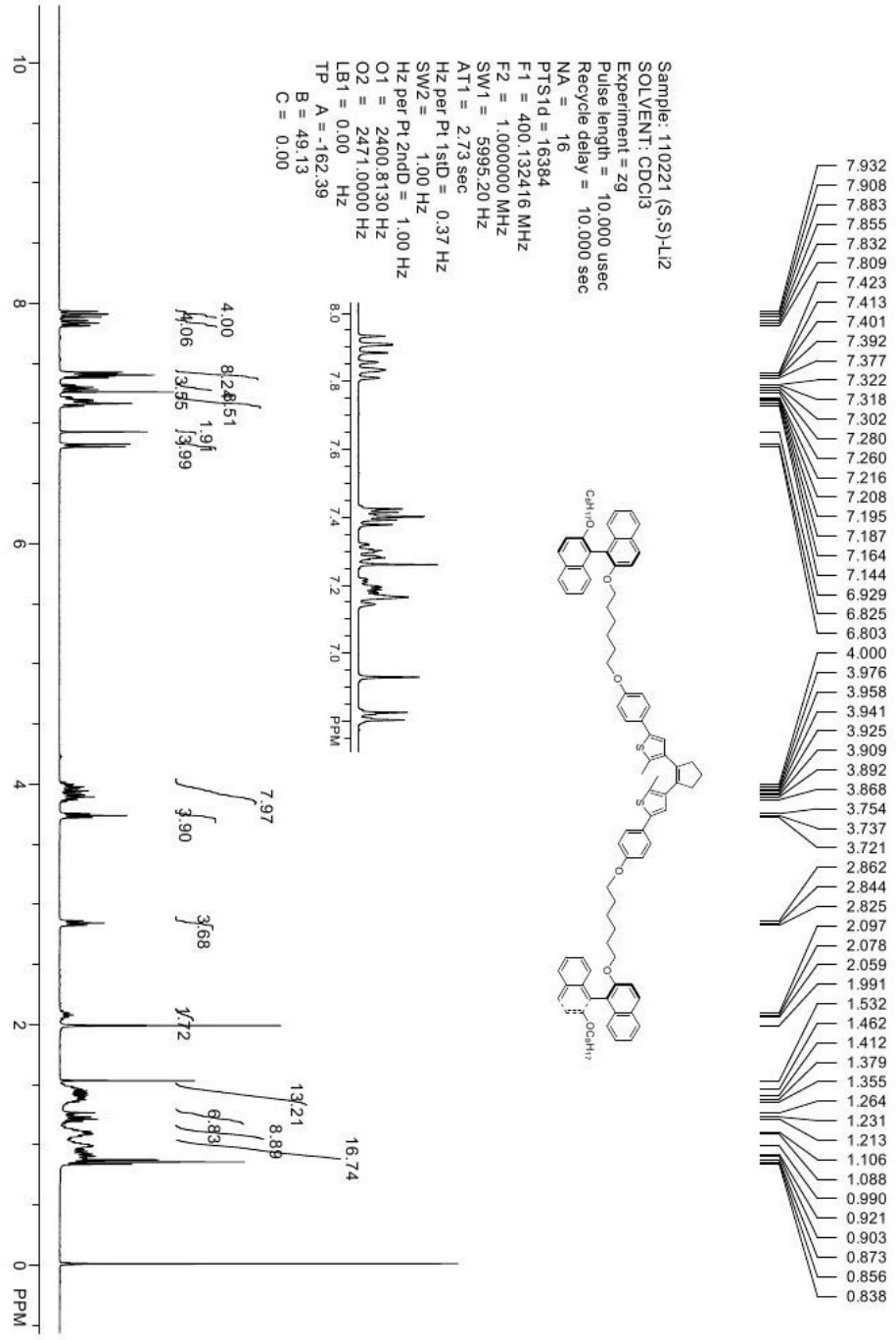

Figure S26. ^{1}H NMR (400 MHz) of (*S*,*S*)-**1a** in $CDCl_3$.

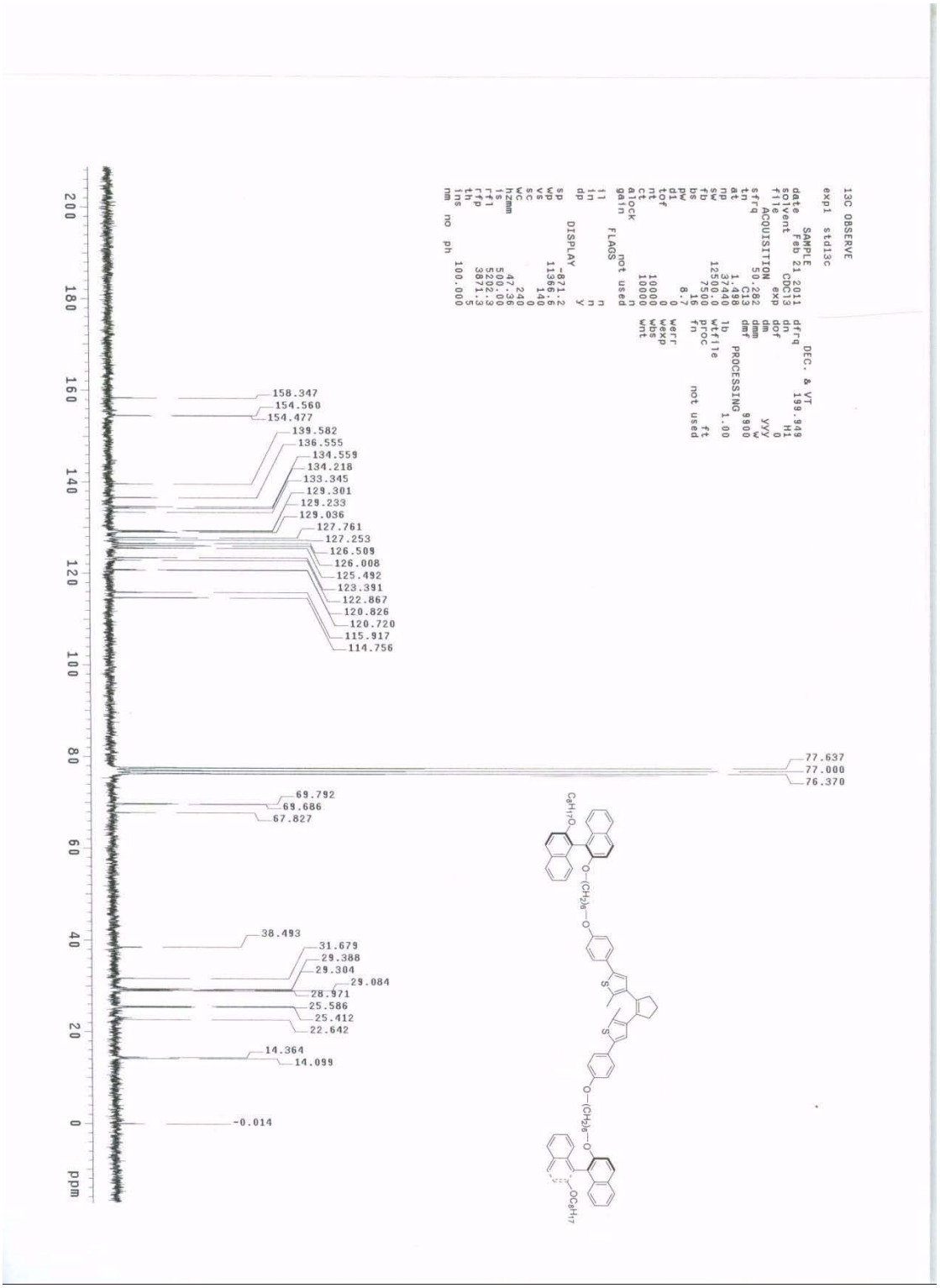

Figure S27. ^{13}C NMR (50 MHz) of (*S*,*S*)-**1a** in $CDCl_3$.

Compound (*R*,*R*)-1b:

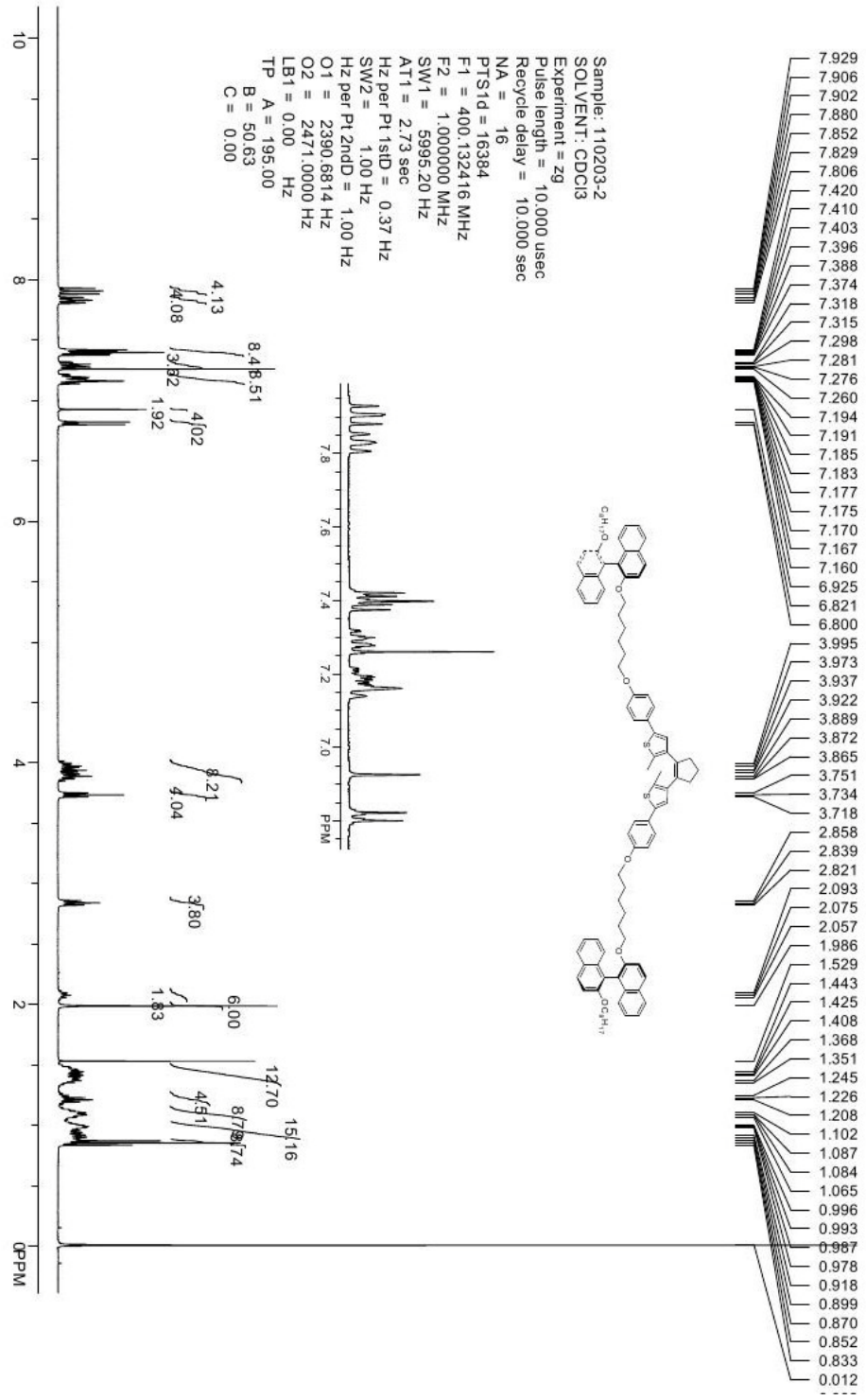

Figure S28. ^{1}H NMR (400 MHz) of (*R*,*R*)-**1b** in $CDCl_3$.

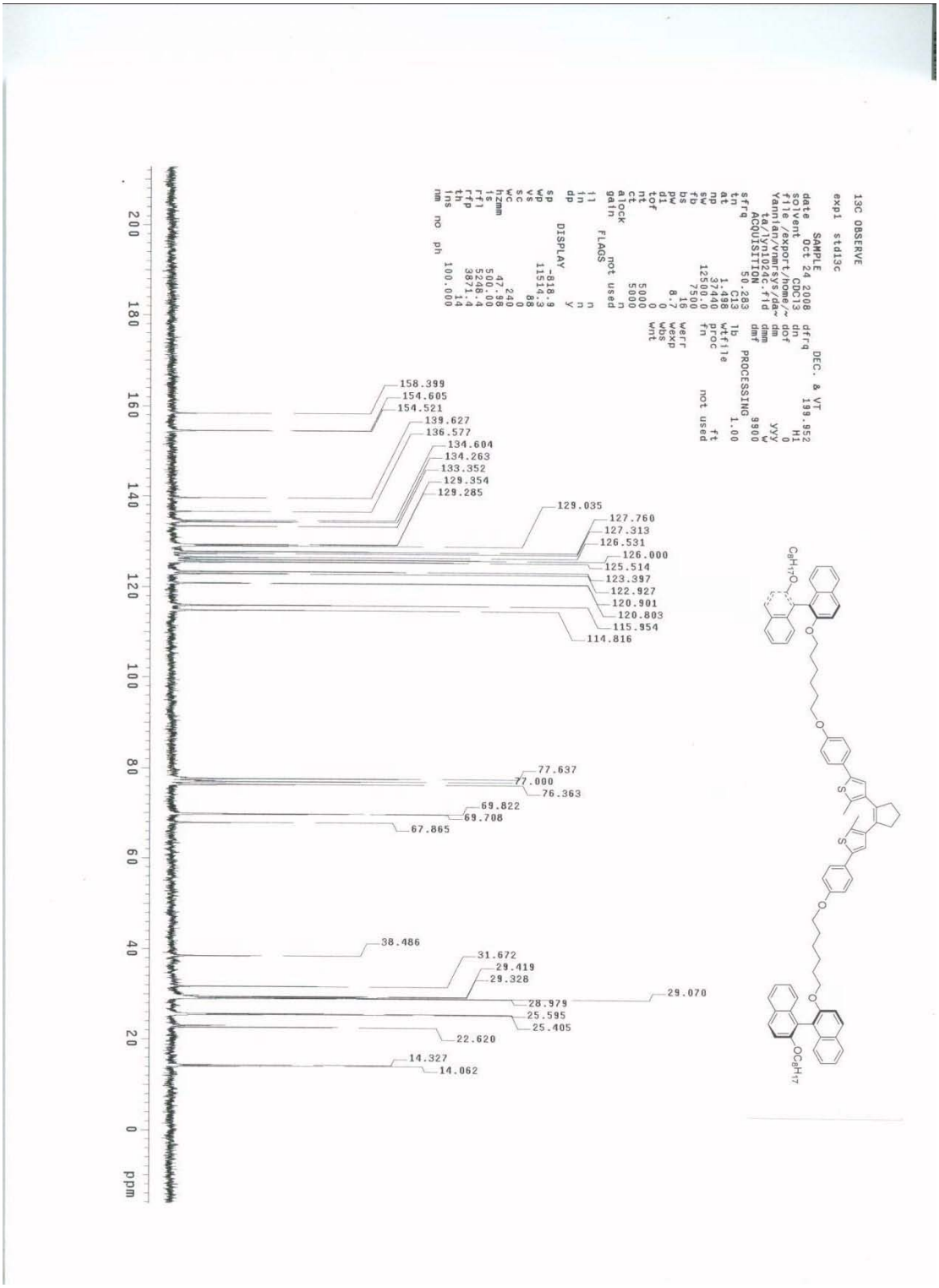

Figure S29. ^{13}C NMR (50 MHz) of (*R*,*R*)-**1b** in $CDCl_3$.

Compound (*S*,*S*)-2:

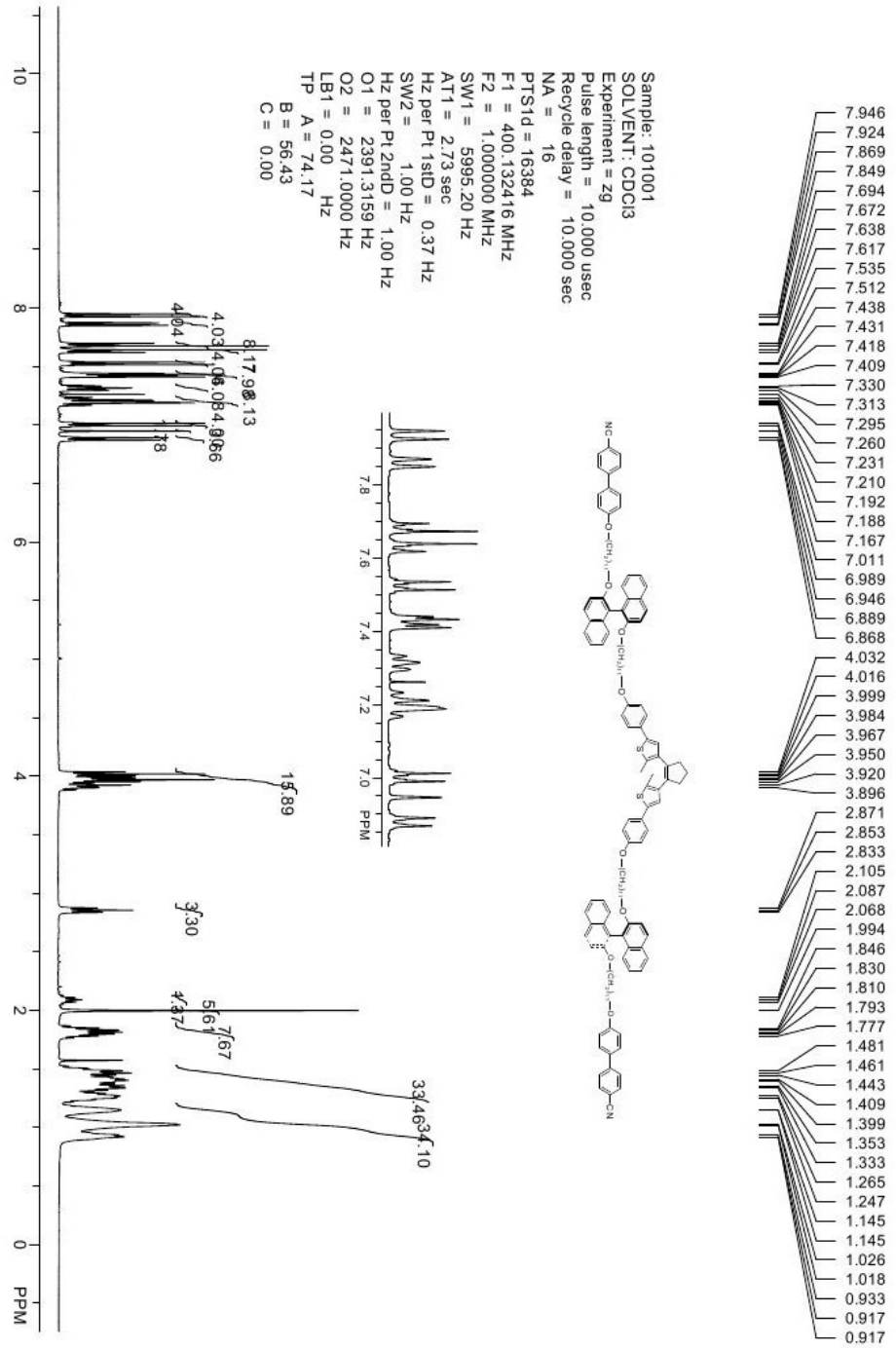

Figure S30. ^{1}H NMR (400 MHz) of (*S*,*S*)-**2** in $CDCl_3$.

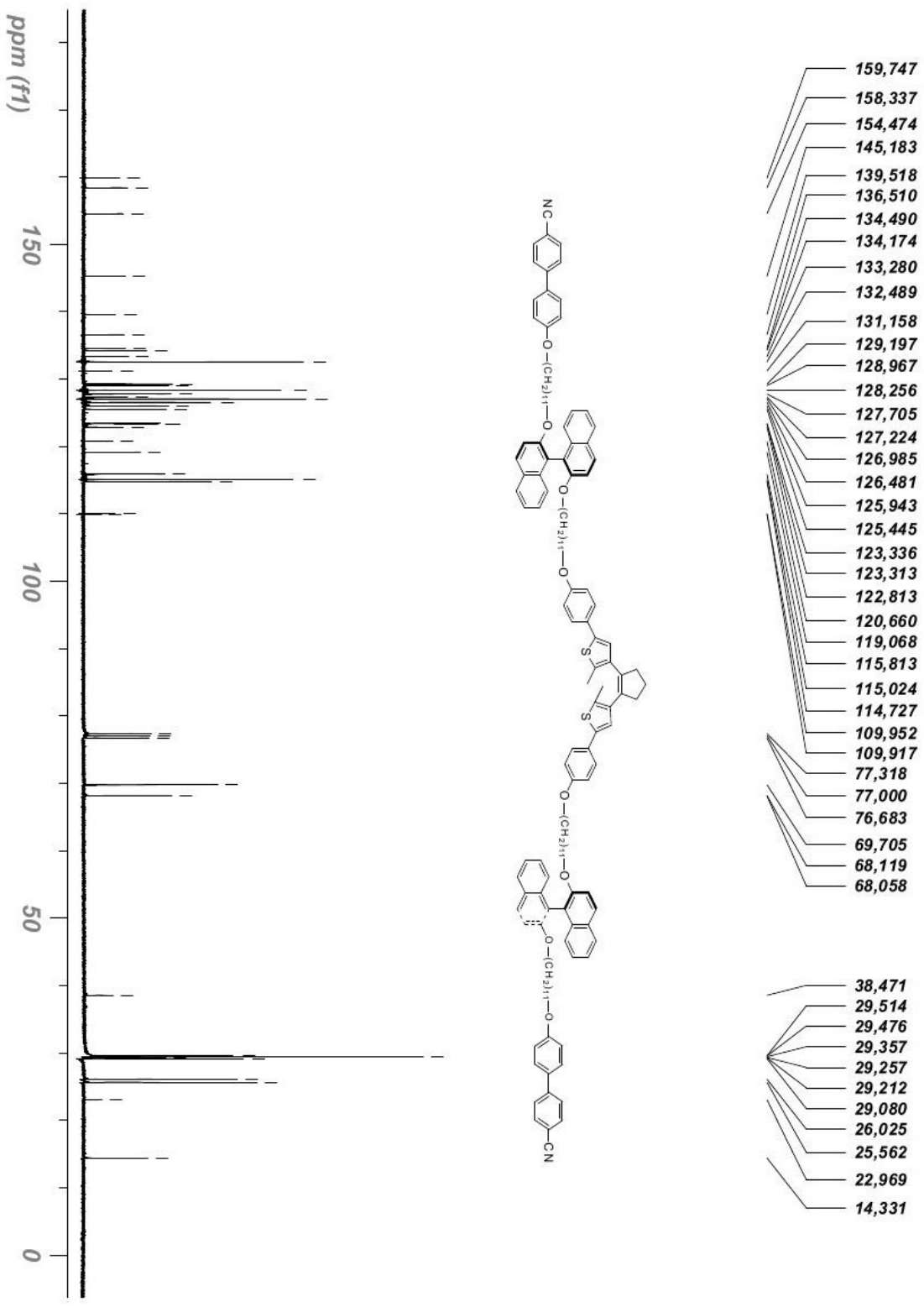

Figure S31. ^{13}C NMR (100 MHz) of (*S*,*S*)-**2** in $CDCl_3$.